ISSN 1024-588X. Вісник Львівського університету. Серія фізична. 2020. Випуск 57. С. 56-64
Visnyk of the Lviv University. Series Physics. 2020. Issue 57. P. 56-64

УДК 535.3; 539.26 https://doi.org/10.30970/vph.57.2020.56
PACS 42.25.Bs; 61.10.Nz; 61.72.Vv

Effect of Dopant Concentration and Crystalline Structure on Absorption Edge of ZnO:Co Films

B. Turko[1], L. Toporovska[1], Y. Eliyashevskyi[1], V. Kapustianyk[1,2], U. Mostovoy[2], Y. Kulyk[1], M. Rudko[1,2]

[1] *Ivan Franko National University of Lviv*
Dragomanova St, 50, 79005 Lviv, Ukraine
e-mail: tyrko_borys@ukr.net

[2] *Scientific-Technical and Education Center of Low Temperature Studies*
Dragomanova St, 50, 79005 Lviv, Ukraine
e-mail: rudko_mykola@ukr.net

We have studied the crystalline structure and absorption spectra for zinc oxide films with different levels of doping with cobalt, deposited by high-frequency magnetron sputtering on the glass substrates. We estimated the concentration of the free charge carriers and showed that the shift of the fundamental absorption edge in ZnO:Co films with dopant level increasing is explained by the Burstein–Moss effect.

Key words: Cobalt-doped zinc oxide, Absorption edge, Optical bandgap, Crystalline Structure, Burstein–Moss effect.

1. Introduction

Cobalt-doped zinc oxide is a promising material for creation of spin-functional devices [1, 2], gas sensors [3, 4], transparent electronics [5], efficient photocatalysts etc. [6]. For optimal application of ZnO:Co films, it is necessary to have in-depth knowledge and understanding of their structure, optical and electrical properties.

For the present day, the mechanism of ferromagnetism in Co-doped ZnO is still under debate due to the formation of secondary phases, segregation or clustering [2, 7].

Some reports in the literature revealed a red-shift in the optical bandgap energy in ZnO:Co with cobalt concentration increasing [5,8–12]. The red-shift is typically attributed to the *sp–d* exchange between the ZnO band electrons and localized *d*-electrons associated with the doping Co^{2+} cations. The interaction leads to corrections in the energy bands; the conduction band is lowered and the valence band is raised causing the bandgap to shrink [13]. On the other hand, other papers have reported a blue-shift in the bandgap

© Turko B., Toporovska L., Eliyashevskyi Y., Kapustianyk V., Mostovoy U., Kulyk Y., Rudko M., 2020

of ZnO with cobalt doping [13–16]. These results indicated that the optical properties are very sensitive to the shape of the samples and to the preparation conditions.

Radio-frequency (RF) magnetron sputtering method is among the best manufacturing techniques of thin oxide films. The method advantages include its suitability for sputtering of high-melting materials, versatility and low cost. The efficiency of RF magnetron sputtering is due to a high activity of the gas component molecules that is stimulated by RF plasma action [17].

In this paper, we present the results of a study of the effect of surface morphology on the optical spectral and electrical properties of thin films of zinc oxide with different levels of doping with cobalt, deposited on glass substrates by a standard RF magnetron sputtering method.

2. Experiment

The films of ZnO:Co (2.0, 4.0, 6.0, 8.0, 10.0 and 12.0 wt. % Co) were obtained by RF magnetron sputtering on glass substrates under an argon atmosphere with working gas pressure 0.1 Pa, high-frequency oscillator power 75 W, distances between target and substrate 60 mm, magnetic field induction 0.1 T, and substrate temperature of 300°C. The target was prepared from a compressed mixture of ZnO (chemically pure grade) and Co_2O_3 (pure grade) powders, used in appropriate proportions. The sputtering time was 200 minutes. According to the ellipsometric measurements data, the thickness of the films was about 2 μm.

The *ex situ* ellipsometry measurements were performed with a serial null ellipsometer LEF-3 M in PCSA (polarizer–compensator–sample–analyzer) arrangement. The light source was He–Ne laser (λ = 632.8 nm).

The X-ray diffraction (XRD) measurements were carried out using STOE STADI P diffractometer with linear position sensitive detector in transmission Bragg-Brentano geometry (Cu $K_{\alpha 1}$ radiation at λ = 0.15406 nm, Ge (111) monochromator, detector scanning step: 0.480° 2θ, accumulation time: 320 s, 2θ angle resolution: 0.015°, 2θrange: 23–115°).

The optical absorption spectra were measured at room temperature on a Specord M-40 spectrophotometer (Germany).

3. Result and discussion

The average crystallite size D of Co-doped ZnO film was calculated using the full width at the half maximum (FWHM) of the (002) diffraction peak and the angle of diffraction θ in Debye-Scherer's formula [17]:

$$D = \frac{0,9\lambda}{\beta \cos\theta}, \tag{1}$$

where λ is the X-ray wavelength, β – FWHM, and θ – Bragg angle of the diffraction peak.

All the samples are found to crystallize in a single phase hexagonal crystal structure. All the peaks are clear, properly indexed and well in agreement with that of standard

Table 1: Some XRD parameters of the ZnO:Co samples

Dopant concentration (wt. %)	h k l	2θ (Degree)		Crystallite size(nm)
		Observed	JCPDS	
2	002	34.41	34.42	69
4	002	34.40	34.42	74
	004	72.73	72.71	
6	002	34.60	34.42	68
	101	36.23	36.25	
	004	72.76	72.71	
8	002	34.22	34.42	74
	101	36.14	36.25	
10	002	34.43	34.42	89
	101	36.27	36.25	
12	002	34.40	34.42	78
	101	36.19	36.25	

datasheet (JCPDS-036-1451) corresponding to the hexagonal wurtzite [14]. For all films, the most intense was the (002) peak. This indicates that all films have preferential c-axis orientation within the (002) plane. For ZnO:Co (6, 8, 10, and 12 wt. %) films, a diffraction (101) peak was observed. No other diffraction peaks related to Co metal or oxides have been detected in any of the doped samples.

The some XRD parameters and the crystalline size of the ZnO:Co samples are shown in Table 1.

Appearance of the structural disorder and decrease of the relative intensity of (002) peak with increasing of doping concentration above 4 wt. % Co can be interpreted as follows. At the low concentrations of Co dopant (less than 4 wt. %) Zn^{2+} ions are replaced by Co^{2+} ions at the crystal lattice sites [16]. Zn and Co are located in the IV period with their atomic numbers 30 and 27 respectively and both have close radii (0.058 nm – for Co and 0.060 nm – for Zn) [14]. Therefore they can substitute each other in the crystals structures [5, 14]. At Co impurity concentrations exceeding 4 wt. %, due to a larger amount of Co, there precede an interstitial incorporation along with the substitutional incorporation of Co [14].

The absorption coefficient α was calculated using the Bouguer–Lambert–Beer formula, based on the transmission spectrum. In the general case, the absorption coefficient is connected with the optical bandgap E_g by the relation [18]:

$$\alpha h\nu = B(h\nu - E_g)^r, \tag{2}$$

where r = 1/2 for the direct allowed transitions; B is a constant that practically is independent of the photon energy.

The values of the optical bandgap were obtained from the dependences of $(\alpha h\nu)^2$ on $h\nu$ in the high absorption region, with extrapolation of the linear sections of the curves to $(\alpha h\nu)^2 = 0$ [18]. Analysis of the fundamental absorption edge using relation (2) shows

that the optical bandgap of undoped ZnO is $E_g = 3.30$ eV (Fig. 1).

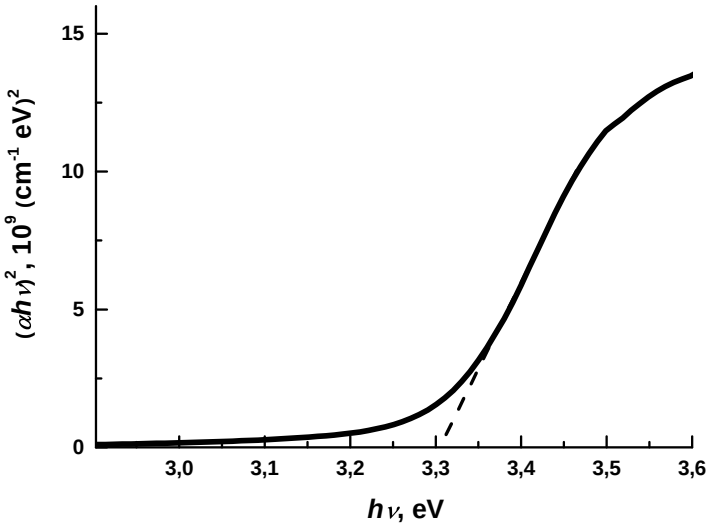

Fig. 1: Absorption spectra in $(\alpha h\nu)^2 = f(h\nu)$ coordinates for 2 μm thick undoped ZnO film obtained at a substrate temperature of 300°C.

Figure 2 shows the absorption spectra in $(\alpha h\nu)^2 = f(h\nu)$ coordinates for ZnO:Co. Using relation (2) and Fig. 2 for ZnO:Co (2, 4, 6, 8, 10 and 12 wt. %) films, we obtained the corresponding values of the optical bandgap: $E_g \approx 3.49$, 3.50, 3.50, 3.66, 3.67, 3.68 eV.

One can suggest that the optical bandgap for ZnO:Co films is larger than for the initial ZnO films because Co^{2+} ions substitute for Zn^{2+} ions at the crystal lattice sites, and interstitial positions are occupied by Co atoms. The increase in optical bandgap of the films due to doping with cobalt according to the conclusions made in report [14] would be explained by the Burstein–Moss effect.

According to the Burstein–Moss effect, expansion of the bandgap in a n-type semiconductor with a parabolic dispersion law for the energy bands due to doping is described by the relation [18]:

$$\Delta E_g = h^2(3\pi^2 n)^{2/3}/(8\pi^2 m^*), \tag{3}$$

where m^* is the effective mass of the electron in the conduction band; h is Planck's constant; n is the carrier concentration. According to this formula, the bandgap increases as the carrier concentration increases.

On the basis of relation (3), we can estimate the concentration of the free charge carriers in ZnO:Co films using two known values of the effective electron mass for ZnO $m^* = 0.24\ m_e$ and $m^* = 0.35\ m_e$ [18]. The results of the calculations are given in Table 2.

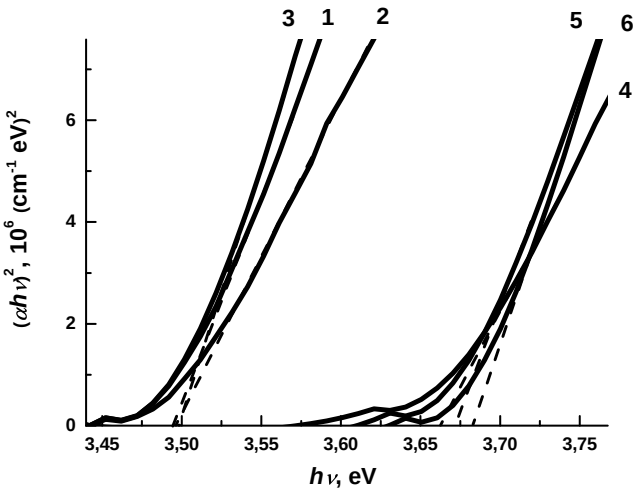

Fig. 2: Absorption spectra in $(\alpha h\nu)^2 = f(h\nu)$ coordinates for ZnO:Co films: C_{Co} = 2(1), 4 (2), 6 (3), 8 (4), 10 (5), and 12 (6) wt. %.

Conclusions

In summary, the films of ZnO and ZnO:Co (2.0, 4.0, 6.0, 8.0, 10.0 and 12.0 wt. % Co) were obtained by RF magnetron sputtering on the glass substrates. According to the ellipsometric measurements data, the thickness of the films was about 2 μm. The crystalline structure and the absorption spectra of these films are investigated. For all the experimental samples, the peak (002) in the X-ray diffraction spectra was the most intense. In the spectra of X-ray diffraction of ZnO:Co (6, 8, 10 and 12 wt%) films beside the intense peak (002), the peak (101) was also observed. For any experimental film samples, no diffraction peaks associated with presence of the metallic cobalt or its oxides were found. The average crystallite sizes in the films calculated using the Debye-Scherer

Table 2: Concentrations of free electrons in ZnO:Co films calculated on the basis of the Burstein–Moss model

Sample	$\Delta E_g, eV$	$n, \times 10^{19} cm^{-3}$ $(m^* = 0.24m_e)$	$n, \times 10^{19} cm^{-3}$ $(m^* = 0.35m_e)$
ZnO:Co (2 wt. %)	0.19	3	5.3
ZnO:Co (4 wt. %)	0.20	3.3	5.7
ZnO:Co (6 wt. %)	0.20	3.3	5.7
ZnO:Co (8 wt. %)	0.26	4.8	8.5
ZnO:Co (10 wt. %)	0.27	5.1	9.0
ZnO:Co (12 wt. %)	0.28	5.4	9.5

formula ranged from 68 nm to 89 nm. In order to explain the phenomenon of structural disorder in ZnO:Co films (6, 8, 10 and 12 wt. %) we suggest that cobalt atoms with concentrations exceeding 4 wt. % not only replace the zinc atoms in their sites in ZnO crystal lattice, but also can occupy the interstitial positions.

We observed a blue shift of the absorption edge of ZnO:Co films with increasing of the cobalt impurity concentration. On the basis of the optical absorption spectra of ZnO and ZnO:Co films (2, 4, 6, 8, 10 and 12 wt. %) analysis the following approximate values of their optical band gap E_g were obtained: 3.30 eV; 3.49 eV; 3.50 eV; 3.50 eV; 3.66 eV; 3.67 eV and 3.68 eV, respectively. The concentration of the free charge carriers in ZnO:Co films turned out to be of the order of 1019 cm^{-3}. It is shown that the shift of the fundamental absorption edge in ZnO:Co films with increasing of the impurity concentration is due to the Burstein–Moss effect.

1. *Ozgur U.* A comprehensive review of ZnO materials and devices / U. Ozgur, Y. Alivov, C. Liu [et al.] // Journal of Applied Physics. – 2005. – Vol. 98. – P. 041301-1–041301-103. https://doi.org/10.1063/1.1992666.
2. *Bellingeri E.* Influence of free charge carrier density on the magnetic behavior of (Zn,Co)O thin film studied by field effect modulation of magnetotransport / E. Bellingeri, S. Rusponi, A. Lehnert [et al.] // Scientific Reports. –2019. – Vol. 9. – P. 149-1–149-12. https://doi.org/10.1038/s41598-018-36336-w
3. *Moosavi F.* Hydrogen sensing properties of Co-doped ZnO nanoparticles / F. Moosavi, M. E. Bahrololoom, R. Kamjou [et al.] // Chemosensors. – 2018. – Vol. 6. – P. 61-1–61-11. https://doi.org/10.3390/chemosensors6040061
4. *Nichev H.* Sensitivity of Co doped ZnO films to NH_3 at room temperature – influence of the deposition temperature / H. Nichev, O. Angelov, J. Pivin [et al.] // Journal of Physics: Conference Series. – 2008. – Vol. 113. – P. 012035-1–012035-4. https://doi.org/10.1088/1742-6596/113/1/012035
5. *Basit M.* Cobalt doping effects on zinc oxide transparent conducting thin films / M. Basit, N. A. Shah, S. M. Ali, A. Zia // World Applied Sciences Journal. – 2014. – Vol. 32. – P. 1664–1670. https://doi.org/10.5829/idosi.wasj.2014.32.08.787
6. *Xu C.* Preparation, characterization and photocatalytic activity of Co-doped ZnO powders / C. Xu, L. Cao, G. Su, W. Liu [et al.] // Journal of Alloys and Compounds. – 2010. – Vol. 497. – P. 373–376. https://doi.org/10.1016/j.jallcom.2010.03.076
7. *Li M.* Structural and optical properties of cobalt doped ZnO nanocrystals / M. Li, J. Xu, X. Chen [et al.] // Superlattices and Microstructures. – 2012. – Vol. 52. – P. 824–833. https://doi.org/10.1016/j.spmi.2012.07.014
8. *Taskin M.* Structural, optical and electrical properties of pure and Co-doped ZnO nano fiber thin films prepared by spray pyrolysis / M. Taskin, J. Podder // App. Sci. Report. – 2015. – Vol. 9. – P. 1–6. https://doi.org/10.15192/PSCP.ASR.2015.9.1.16
9. *Kaphle A.* Doping efficiency in cobalt-doped ZnO nanostructured materials / A. Kaphle, T. Reed, A. Apblett, P. Hari // Journal of Nanomaterials. – 2019. – Vol. 2019. – P. 7034620-1–7034620-13. https://doi.org/10.1155/2019/7034620

10. *Khantoul A. R.* Structural and optical properties of ZnO and Co doped ZnO thin films prepared by sol-gel / A. R. Khantoul, M. Sebais, B. Rahal [et al.] // Acta Physica Polonica A. – 2018. – Vol. 133. – P. 114–117. https://doi.org/10.12693/APhysPolA.133.114
11. *Gandhi V.* Effect of cobalt doping on structural, optical, and magnetic properties of ZnO nanoparticles synthesized by coprecipitation method / V. Gandhi, R. Ganesan, H. H. A. Syedahamed, M. Thaiyan // Journal of Physical Chemistry C. – 2014. – Vol. 118 – P. 9715–9725. https://doi.org/10.1021/jp411848t
12. *Savchuk A. I.* Structural and optical properties of $Zn_{1-x}Co_xO$ thin films prepared by RF reactive sputtering technique / A. I. Savchuk, I. D. Stolyarchuk, I. Stefaniuk [et al.] // Semiconductor Physics, Quantum Electronics & Optoelectronics. – 2014. – Vol. 17. – P. 353–357. https://doi.org/10.15407/spqeo17.04.353
13. *Ivill M.* Structure and magnetism of cobalt-doped ZnO thin films / M. Ivill, S. J. Pearton, S. Rawal [et al.] // New Journal of Physics. – 2008. – Vol. 10. – P. 065002-1–065002-21. https://doi.org/10.1088/1367-2630/10/6/065002
14. *Chanda A.* Study of structural, optical and magnetic properties of cobalt doped ZnO nanorods / A. Chanda, S. Gupta, M. Vasundhara [et al.] // RSC Adv. – 2017. – Vol. 7. – P. 50527–50536. https://doi.org/10.1039/c7ra08458g
15. *Benramache S.* Study on the correlation between crystallite size and optical gap energy of doped ZnO thin film / S. Benramache, A. Arif, O. Belahssen, A. Guettaf // Journal Of Nanostructure in Chemistry. – 2013. – Vol. 3. – P. 80-1–80-6. https://doi.org/10.1186/2193-8865-3-80
16. *Benramache S.* Preparation of transparent, conductive ZnO:Co and ZnO:In thin films by ultrasonic spray method / S. Benramache, B. Benhaoua, H. Bentrah // Journal Of Nanostructure in Chemistry. – 2013. – Vol. 3. – P. 54-1–54-7. https://doi.org/10.1186/2193-8865-3-54
17. *Panasyuk M. R.* Manufacturing technology, optical and spectral properties of nanostructurized thin ZnO films / M. R. Panasyuk, B. I. Turko, V. B. Kapustianyk [et al.] // Functional Mater. 2005. Vol. 12. P. 746–749. http://functmaterials.org.ua/contents/12-4/fm124-26.pdf
18. *Kapustianyk V. B.* Effect of dopants and surface morphology on the absorption edge of ZnO films doped with In, Al, and Ga / V. B. Kapustianyk, B. I. Turko, V. P. Rudyk [et al.] // Journal of Applied Spectroscopy. – 2015. – Vol. 82. P. 153 156. https://doi.org/10.1007/s10812-015-0079-y

References

1. U. Ozgur, Y. Alivov, C. Liu, A. Teke, M.A. Reshchikov, S. Dogan, V. Avrutin, S.-J. Cho, H. Morkoç, Journal of Applied Physics. **98**, 041301-1–041301-103 (2005). doi:10.1063/1.1992666.
2. E. Bellingeri, S. Rusponi, A. Lehnert, H. Brune, F. Nolting, A. Leveratto, A. Plaza and D. Marré, Scientific Reports. **9**, 149-1–149-12 (2019). doi:10.1038/s41598-018-36336-w.
3. F. Moosavi, M.E. Bahrololoom, R. Kamjou, A. Mirzaei, S.G. Leonardi and G. Neri, Chemosensors. **6**, 61-1–61-11 (2018). doi:10.3390/chemosensors6040061.
4. H. Nichev, O. Angelov, J. Pivin, R. Nisumaa and D. Dimova-Malinovska, Journal

of Physics: Conference Series. **113**, 012035-1–012035-4 (2008). doi:10.1088/1742-6596/113/1/012035.

5. M. Basit, N.A. Shah, S.M. Ali, A. Zia, World Applied Sciences Journal. **32**, 1664–1670 (2014). doi:10.5829/idosi.wasj.2014.32.08.787.
6. C. Xu, L. Cao, G. Su, W. Liu, X. Qu, Y. Yu, Journal of Alloys and Compounds. **497**, 373–376 (2010). doi:10.1016/j.jallcom.2010.03.076.
7. M. Li, J. Xu, X. Chen, X. Zhang, Y. Wu, P. Li, X. Niu, Ch. Luo, L. Li, Superlattices and Microstructures. **52**, 824–833 (2012). doi:10.1016/j.spmi.2012.07.014.
8. M. Taskin, J. Podder, App. Sci. Report. **9**, 1–6 (2015). doi:10.15192/PSCP.ASR.2015.9.1.16.
9. A. Kaphle, T. Reed, A. Apblett, P. Hari, Journal of Nanomaterials. **2019**, 7034620-1–7034620-13 (2019). doi:10.1155/2019/7034620.
10. A.R. Khantoul, M. Sebais, B. Rahal, B. Boudine, O. Halimi, Acta Physica Polonica A. **133**, 114–117 (2018). doi:10.12693/APhysPolA.133.114.
11. V. Gandhi, R. Ganesan, H.H.A. Syedahamed, M. Thaiyan, Journal of Physical Chemistry C. **118**, 9715–9725 (2014). doi:10.1021/jp411848t.
12. A.I. Savchuk, I.D. Stolyarchuk, I. Stefaniuk, B. Cieniek, E. Sheregii, Semiconductor Physics, Quantum Electronics & Optoelectronics. **17**, 353–357 (2014). doi:10.15407/spqeo17.04.353.
13. M. Ivill, S.J. Pearton, S. Rawal, L. Leu, P. Sadik, R. Das, A.F. Hebard, M. Chisholm, J.D. Budai and D.P. Norton, New Journal of Physics. **10**, 065002-1–065002-21 (2008). doi:10.1088/1367-2630/10/6/065002.
14. A. Chanda, S. Gupta, M. Vasundhara, Sh.R. Joshi, G.R. Muttae and J. Singh, RSC Adv. **7**, 50527–50536 (2017). doi:10.1039/c7ra08458g.
15. S. Benramache, A. Arif, O. Belahssen, A. Guettaf, Journal Of Nanostructure in Chemistry. **3**, 80-1–80-6 (2013). doi:10.1186/2193-8865-3-80.
16. S. Benramache, B. Benhaoua, H. Bentrah, Journal Of Nanostructure in Chemistry. **3**, 54-1–54-7 (2013). doi:10.1186/2193-8865-3-54.
17. M.R. Panasyuk, B.I. Turko, V.B. Kapustianyk, G.A. Lobochkova, V.P. Rudyk, A.P. Vaskiv, V.M. Davydov, Functional Mater. **12**, 746–749 (2005). http://functmaterials.org.ua/contents/12-4/fm124-26.pdf.
18. V.B. Kapustianyk, B.I. Turko, V.P. Rudyk, B.Y. Kulyk, M.S. Rudko, Journal of Applied Spectroscopy. **82**, 153–156 (2015). doi:10.1007/s10812-015-0079-y

Статтю отримано: 13.10.2020
Прийнято до друку: 16.12.2020

Вплив концентрації легуючих домішок і кристалічної структури на край поглинання плівок ZnO:Co

Б. Турко[1], Л. Топоровська[1], Ю. Еліяшевський[1], В. Капустяник[1,2], У. Мостовой[2], Ю. Кулик[1], М. Рудко[1,2]

[1] *Львівський національний університет імені Івана Франка*
вул. Драгоманова, 50, 79005 Львів, Україна
e-mail: tyrko_borys@ukr.net

[2] *Науково-технічний і навчальний центр низькотемпературних досліджень*
вул. Драгоманова, 50, 79005 Львів, Україна
e-mail: rudko_mykola@ukr.net

Методом високочастотного магнетронного розпилення на скляних підкладках в атмосфері робочого газу аргону за тиску 0,1 Па, потужності генератора високочастотних коливань 75 Вт, індукції магнітного поля 0,1 Тл, відстані між мішенню та підкладкою 6 см та за температури підкладок 300°C, отримано плівки ZnO і ZnO:Co (2, 4, 6, 8, 10 і 12 ваг. %) завтовшки 2 мкм. Досліджено кристалічну структуру та спектри поглинання цих плівок. Для усіх експериментальних зразків найбільш інтенсивним у спектрах дифракції X-променів був пік (002). У спектрах дифракції X-променів плівок ZnO:Co (6, 8, 10 і 12 ваг. %), окрім інтенсивного піку (002), спостерігався ще й пік (101). Для жодного з експериментальних плівкових зразків не виявлено дифракційних піків, пов'язаних з наявністю металічного кобальту чи його оксидів. Розраховані за формулою Дебая–Шерера середні розміри кристалітів у плівках були у діапазоні від 68 до 89 нм. Для пояснення явища структурного розупорядкування в плівках ZnO:Co (6, 8, 10 і 12 ваг. %) висловлено гіпотезу, про те, що атоми кобальту при концентраціях легуючої домішки, вищих за 4 ваг. %, не лише заміщають атоми цинку у вузлах кристалічної ґратки ZnO, а й починають займати міжвузлові позиції. З підвищенням концентрації домішки кобальту спостерігалося зміщення краю поглинання плівок ZnO:Co в короткохвильову область спектра. На основі проведеного аналізу спектрів оптичного поглинання плівок ZnO та ZnO:Co (2, 4, 6, 8, 10 і 12 ваг. %) було отримано приблизні значення їхніх оптичних ширин заборонених зон Eg: 3,30 еВ; 3,49 еВ; 3,50 еВ; 3,50 еВ; 3,66 еВ; 3,67 еВ та 3,68 еВ, відповідно. Концентрація вільних носіїв заряду у плівках ZnO:Co виявилася порядку 10^{19} см$^{-3}$. Продемонстровано, що зсув краю фундаментального поглинання у плівках ZnO:Co під час збільшення концентрації домішки зумовлений ефектом Бурштейна–Мосса.

Ключові слова: легований кобальтом оксид цинку, край поглинання, оптична ширина забороненої зони, кристалічна структура, ефект Бурштейна–Мосса.